ACCSCIENCE PUBLISHING

International Journal of Bioprinting

REVIEW ARTICLE

In situ bioprinting: Control strategies, bioinks, applications, challenges, and future perspectives

Zijun Zheng[1†], Xinrong Tan[1†], Huixin Liang[2,3], Lan Li[2,3*], Qing Jiang[2,3*], and Jianping Shi[1*]

[1]School of Electrical Engineering and Automation, Nanjing Normal University, Nanjing, Jiangsu, China

[2]State Key Laboratory of Pharmaceutical Biotechnology, Division of Sports Medicine and Adult Reconstructive Surgery, Department of Orthopedic Surgery, Branch of National Clinical Research Center for Orthopedics, Drum Tower Hospital Affiliated to Medical School of Nanjing University, Nanjing, Jiangsu, China

[3]Jiangsu Engineering Research Center for 3D Bioprinting, Nanjing, Jiangsu, China

Abstract

In situ bioprinting is an emerging technology that directly deposits bioinks on demand within clinical environments to generate targeted tissue structures. It integrates the printing and implantation processes, allowing the printed constructs to interact directly with the host biological microenvironment. This technology reduces the risk of contamination during transplantation and improves operational precision, thus demonstrating broad application prospects in fields such as tissue repair and biomedical sensor fabrication. This article discusses the following aspects: (i) from the perspective of control strategies, it summarizes the developmental trend of *in situ* bioprinting from open-loop control toward closed-loop control, and outlines key procedures including geometric reconstruction, conformal slicing, infill trajectory planning, and parameter mapping in *in situ* bioprinting; (ii) with reference to body-surface and open-exposure scenarios, minimally invasive intervention scenarios, remote energy-driven scenarios, and biosensing scenarios, this review discusses the demands faced by *in situ* bioprinting in different application settings, the design logic of bioinks, and representative research progress; (iii) the printable characteristics and application boundaries of natural polymers, synthetic polymers, and 4D smart materials in *in situ* bioprinting are summarized. Finally, the challenges faced by this technology and its potential directions for improvement in the future are also discussed.

Keywords: *In situ* bioprinting; Control strategy; Actuation system; Bioinks; Application scenarios

†*These authors contributed equally to this work.*

***Corresponding authors:**
Lan Li
(lanl17@163.com)
Qing Jiang
(qingj@nju.edu.cn)
Jianping Shi
(jpshi@njnu.edu.cn)

Citation: Zheng Z, Tan X, Liang H, Li L, Jiang Q, Shi J. *In situ* bioprinting: Control strategies, bioinks, applications, challenges, and future perspectives. *Int J Bioprint.* 2026;12(3):026200196. doi: 10.36922/IJB026200196

Received: March 23, 2026

Revised: May 15, 2026

Accepted: May 27, 2026

Published online: May 29, 2026

1. Introduction

In situ bioprinting can be defined as a technology that directly patterns bioinks within clinical environments to generate tissue structures with the desired volumetric geometry.[1] As an advanced biomanufacturing strategy, *in situ* bioprinting integrates the deposition process of cells and biomaterials with clinical intervention procedures, enabling the direct construction of tissue structures *in vivo* or on body surfaces. Through

this approach, the printed structures can be immediately exposed to the physiological microenvironment of the host after formation, achieving *in situ* maturation under the synergistic effects of blood supply, immune regulation, and mechanical signals, thereby promoting tissue integration and functional recovery.[2,3] Meanwhile, this strategy avoids complex *in vitro* culture and transportation processes, helping to reduce the risk of exogenous contamination and improve the precision of spatial positioning and morphological matching between the constructed structures and target tissues.

From the perspective of technical systems, three-dimensional (3D) bioprinting can mainly be classified into extrusion-based, inkjet-based, and photocuring-based approaches according to their forming principles. Extrusion-based bioprinting achieves material deposition through continuous extrusion and exhibits good adaptability to high-viscosity bioinks and high-cell-density systems.[4] Inkjet-based bioprinting enables high-resolution deposition in the form of droplets, but it requires strict control over material viscosity and environmental stability.[5,6] Photocuring-based bioprinting relies on photocrosslinking reactions for rapid fabrication, offering high precision but showing strong dependence on material systems and operational conditions.[7-9] To meet the demand for stable deposition in complex and dynamic environments during *in situ* bioprinting, extrusion-based technology has become the predominant implementation approach due to its relatively simple system architecture, broad compatibility with bioinks, and ease of handheld operation or integration with robotic arms. Inkjet-based technology demonstrates certain potential in scenarios requiring precise deposition, and inkjet-based bioprinting has been applied in bone and skin repair. However, its stringent bioink requirement and potential effects on encapsulated cells may limit its suitability for organ repair.[10,11] Photocuring-based technology is limited in *in situ* bioprinting applications because of its dependence on optical pathways and operational space. In most cases, bioinks are first extruded and subsequently irradiated with an external ultraviolet lamp on a platform. Nevertheless, vat photopolymerization technology is expected to overcome some of the application limitations.[12,13]

In terms of implementation mechanisms, *in situ* bioprinting generally requires material deposition to be performed on non-ideal and dynamically changing substrates. The printing region exhibits continuous variations in spatial posture and Z-axis height, which impose higher requirements on the motion control, path planning, and real-time feedback capabilities of the printing system. In addition, during *in vivo* repair processes, target tissues undergo movement and deformation caused by physiological rhythms such as respiration, pulsation, and changes in muscle tension, resulting in printing surfaces that are typically freeform and time-varying.[14] These characteristics have driven the development of control strategies in *in situ* bioprinting from traditional open-loop control toward closed-loop control based on perceptual feedback.

The applicability of *in situ* bioprinting is closely related to the anatomical location and accessibility of the target tissue. From the perspective of application scenarios, this strategy has been extensively explored in superficial tissue repair, such as skin wounds, cartilage, and bone defects. These tissues have favorable visualization conditions and operational accessibility and are usually treated in open environments, enabling high-precision deposition. On the other hand, with the development of flexible printing devices, minimally invasive platforms, and endoscopic-assisted systems, *in situ* bioprinting has also shown potential applications in internal organs such as the liver and stomach wall. For example, biomaterials and cells can be precisely deposited at injury sites through minimally invasive platforms to promote local tissue regeneration. It is noteworthy that, compared with superficial tissues, internal organ environments are significantly more dynamic and complex.[15-18] Taking the liver as an example, liver tissue is characterized by high vascularization, a complex mechanical environment, and continuous physiological motion, all of which impose higher demands on path planning, deposition stability, and real-time feedback control of printing systems. For visceral organs such as the liver, repair in an open environment is feasible; however, it requires a large surgical incision. Minimally invasive surgery, by contrast, can accomplish the same task through a small incision and is more conducive to postoperative recovery. In this scenario, the system only needs to "puncture" the actuator into the body and then autonomously complete the repair process. However, how to achieve accurate positioning and motion control of the actuator under puncture conditions remains a challenging problem. Therefore, although current *in situ* bioprinting has shown potential for expansion toward deep tissues, its applications are still under active development. In addition, *in situ* bioprinting provides a new paradigm for the on-site fabrication of wearable and implantable biosensors. For example, flexible electrodes, conductive hydrogels, and strain-sensing structures can be directly printed at wound sites to enable continuous monitoring of tissue healing, infection status, or local mechanical environments.[19-22]

In situ bioprinting is an interdisciplinary research field that integrates control strategies, bioinks, printing systems,

and sensing technologies. This paper reviews the research progress of *in situ* bioprinting in terms of control strategies, algorithms, application scenarios, and bioinks, and further discusses its future development directions.

2. Control strategies and algorithms for *in situ* bioprinting

2.1. Control strategies

Zhu *et al.*[23] classified *in situ* bioprinting into open-loop printing and closed-loop printing. Accordingly, control strategies can also be divided into open-loop control strategies and closed-loop control strategies. Open-loop control relies on preoperative modeling and predefined path execution, without real-time correction based on environmental changes during the printing process. In contrast, closed-loop control continuously senses the target state through a feedback system composed of sensors and uses the feedback information in real time for trajectory correction and parameter adjustment, thereby improving the system's adaptability to dynamic environments during the printing process.

2.1.1. Open-loop control strategy

Open-loop control is an earlier adopted control mode in *in situ* bioprinting. Its basic idea is to complete geometric acquisition of the target region, path planning, and printing parameter setting before printing, and then perform material deposition according to a pre-generated trajectory during the printing process. This strategy typically includes steps such as preoperative imaging, 3D model reconstruction, defect modeling, offline path planning, and trajectory execution. Its characteristics include a relatively simple system architecture and clear control logic, making it suitable for printing scenarios where the target position is stable and morphological changes are minimal.

Cohen *et al.*[24] used a 3D printer based on a three-axis gantry motion system. By performing Boolean operations on computed tomography (CT) images acquired before and after defect creation, they generated a defect model and successfully completed the repair of osteochondral defects, with outcomes meeting clinically acceptable standards. Li *et al.*[25] employed a modified four-degree-of-freedom robotic arm to perform repair printing on porcine bone defects and established a robotic arm error model and kinematic model to compensate for *ex vivo* printing errors. Specifically, recognition and compensation were introduced into the defect model, ultimately reducing the average error to 0.5157 ± 0.4240 mm. The system completed tibial defect repair within 12 minutes and achieved superior tissue regeneration quality during the postoperative recovery phase. The above studies indicate that open-loop control can achieve relatively high precision during *in situ* construction by relying on compensation methods to reduce errors under conditions where geometric information is accurate and the target region is relatively stable.

However, the limitation of open-loop control lies in its strong dependence on the accuracy of preoperative modeling and the precision of predefined paths. When the target tissue undergoes displacement, deformation, or posture changes during the printing process, the system cannot promptly correct trajectory deviations, which may easily lead to deposition mismatch, structural deformation, or even printing failure. Therefore, open-loop control is more suitable for relatively stable printing scenarios such as bone and cartilage, while its adaptability is limited in motile tissues and complex *in vivo* environments.

2.1.2. Closed-loop control strategy

Closed-loop control is a further development based on open-loop control, and its core feature is the introduction of a feedback system during the printing process, enabling the execution system to dynamically correct the printing process according to changes in the target state. Unlike the asynchronous mode of planning and execution in open-loop control, planning and execution in closed-loop control are synchronized, and the system is typically composed of a sensing module, a state estimation module, a control decision-making module, and an execution module. This strategy can perceive in real time the geometric changes of the printing surface, deformation states, and the relative relationship between the nozzle and the surface, and accordingly dynamically adjust the printing trajectory, nozzle height, or printing parameters, thereby improving the stability and precision of *in situ* printing in dynamic environments.

O'Neill *et al.*[26] designed an early closed-loop printing strategy. The team used a hand-tracking sensor, a laser profilometer, a custom software stack, and a three-degree-of-freedom robot to track a moving hand and print predefined geometries onto unfixed and dynamic substrates using piezoelectric microjet technology. Kucukdeger and Johnson[27] achieved planar and non-planar additive manufacturing on moving substrates and objects through real-time sensing of local object–tool offsets. Specifically, they employed a process-integrated one-dimensional laser displacement sensor to locally monitor the nozzle–surface offset, thereby enabling real-time control of the z-axis position of the microextrusion nozzle. Finally, a three-axis robot was used to accomplish *in situ* conformal additive manufacturing of single-layer and multilayer hydrogel structures on a vertically moving adult hand.

In the field of *in situ* bioprinting for biological tissues, Zhu *et al.*[28] designed a computer vision-assisted integrated robotic system to achieve adaptive printing. This system acquired surface information via structured-light scanning and combined it with real-time estimations of the rigid-body motion of the target surface. The integrated feedback was then transmitted to the motion controller to realize adaptive printing. Finally, the system was integrated with an extrusion-based 3D printer for two experiments: first, the strategy was validated by directly fabricating high-performance and easily removable wirelessly powered electronic devices on unconstrained human hands; and second, repair was performed on mouse skin wounds, demonstrating the feasibility of *in situ* bio-repair applications.

Furthermore, Zhu *et al.*[29] proposed another closed-loop bioprinting system integrating artificial intelligence (AI). They used a structured-light 3D scanner to construct an offline learning point cloud dataset and a pair of synchronized machine vision cameras to perform 3D tracking of reference markers. Subsequently, a 3D bioprinting gantry system was used to print electrical impedance tomography (EIT) sensors on periodically contracting porcine lungs, achieving *in situ* monitoring of lung deformation. Derayatifar *et al.*[30] also incorporated AI algorithms into the closed-loop control strategy. In their previous studies on direct sound printing (DSP), the team found that although the conventional iterative angular spectrum approach could effectively reconstruct target acoustic patterns, it exhibited significant limitations in efficiency and practical feasibility. Therefore, they introduced penalty functions and deep learning algorithms into the reconstruction process to rapidly and accurately reconstruct holographic images. The results showed that the uniformity of the final printed parts was improved, alleviating the thickening problem of partially cured components before the completion of printing. Discussions regarding applications in the field of biosensing and other studies on DSP will be presented in subsequent sections. Figure 1 presents two closed-loop control strategies applied in *in situ* bioprinting.

For deep-tissue and minimally invasive scenarios, Zhao *et al.*[31] proposed a closed-loop *in situ* printing strategy suitable for minimally invasive surgery. Specifically, they developed a novel binary chromatic ring array marker for robust trocar recognition, which enables precise localization and pose estimation of the trocar. This marker, together with a seven-degree-of-freedom bioprinting robot, constituted a closed-loop system. To make the printing robot's kinematics an adaptive closed-loop system, they introduced fixed red–green–blue-depth (RGB-D)-based visual servo control. Using this system, the team achieved 3D bioprinting for lesion resection and tissue repair on curved surfaces of porcine liver tissue via minimally invasive procedures, achieving accurate deposition on curved porcine liver surfaces and maintaining minimal contact force at the incision site.

2.2. Path planning and slicing algorithms

In situ bioprinting usually needs to deal with real tissue surfaces that are irregular, non-planar, deformable, and often subject to physiological motion. Therefore, its path generation process must not only satisfy geometric filling requirements, but also take into account surface conformity and deposition continuity. This poses challenges for printing path planning. In general, path planning in *in situ* bioprinting typically includes four major steps: geometric reconstruction of the defect region, generation of slicing strategies, infill trajectory planning, and mapping of printing parameters.

2.2.1. Geometric reconstruction and defect modeling

The prerequisite for path planning is the acquisition of 3D geometric information of the target region. For stable tissues such as bone and cartilage, volumetric data of the defect region are usually obtained through CT, cone-beam computed tomography, or magnetic resonance imaging, followed by 3D reconstruction and extraction of defect boundaries. In contrast, for soft tissue scenarios such as skin and visceral organs, surface information is more commonly acquired in real time using structured-light scanning, laser profilometry, binocular vision, or RGB-D sensors.[32] Subsequently, 3D models of the target printing region are generated through point cloud registration, surface fitting, and mesh reconstruction, thereby providing the basis for subsequent slicing and path planning.

2.2.2. Slicing algorithms

Slicing is a key step in converting a 3D target model into executable printing trajectories. Its core task is to decompose the target region into a series of two-dimensional or quasi-two-dimensional paths that can be deposited layer by layer. For *in situ* bioprinting, because the target surface often exhibits significant curvature or even dynamic fluctuations, traditional planar slicing can easily lead to interlayer mismatch, frequent nozzle lifting, and nonuniform deposition. Therefore, the concept of "conformal" slicing has emerged.

Alkadi *et al.*[33] investigated conformal 3D slicing algorithms. In their study, "layers" were no longer treated as planar surfaces; instead, they redefined a "layer" as a set of conformal slicing surfaces generated by progressively offsetting along the normal direction of the substrate

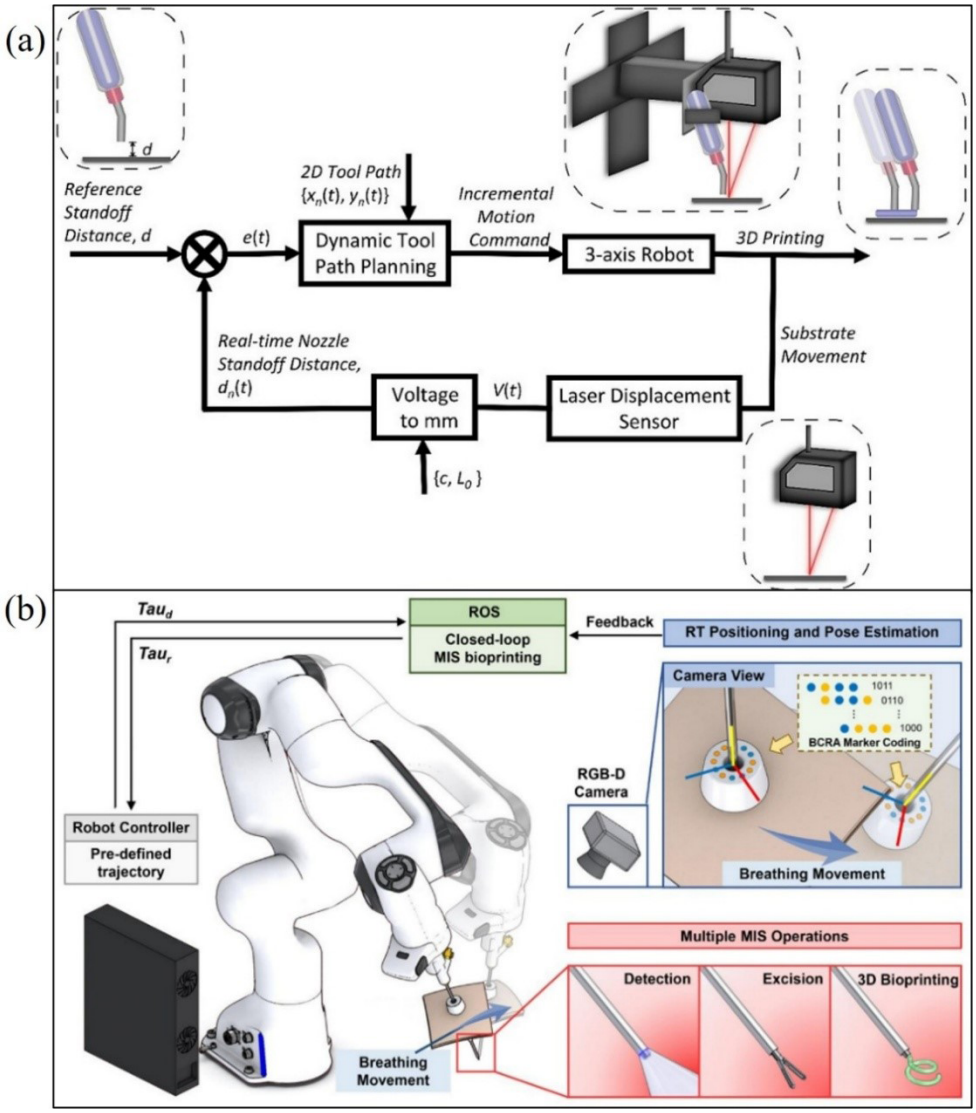

Figure 1. Sensing device-based closed-loop control strategies for *in situ* bioprinting. (a) Closed-loop control strategy based on a one-dimensional laser displacement sensor, in which the distance between the nozzle and the printing surface is adjusted by comparing the measured values of the laser sensor with the reference values, thereby improving the printing effect. Reprinted with permission from Kucukdeger and Johnson.[27] Copyright © 2023 Elsevier Inc; (b) Visual-recognition-based closed-loop *in situ* bioprinting strategy using a trocar needle; the system adjusts the trocar pose based on the color-ring numbers collected by the vision camera, where a group of four consecutive marking points is assigned a specific number. Reprinted with permission from Zhao *et al.*[31] Copyright © 2023 Elsevier Inc.

Abbreviations: BCRA: Binary chromatic ring array; MIS: Minimally invasive surgery; RGB-D: Red–green–blue-depth; ROS: Robot operating system; RT: Real-time.

surface. In this way, a series of non-planar slicing surfaces consistent with the substrate morphology was constructed, enabling the printing path of each layer to conform to the continuously varying geometry of the target surface.

Ji *et al.*[34] proposed a conformal algorithm capable of fabricating 3D structures on freeform curved substrates without parameterizing the substrate surface or modifying the geometric design of the printed structure. Unlike the approach of Alkadi *et al.*,[33] they first extracted the top-layer contour and surface height information from the conventional slicing paths of the substrate and represented them as a height mapping function H(x,y) on a two-dimensional plane. Subsequently, the target structure was sliced, and the Z-coordinates of all path points were compensated by adding the values of H(x,y) corresponding to their X and Y coordinates. This slicing method does not require extensive computational resources; however, it

cannot guarantee a safe distance between the nozzle and the substrate. The detailed slicing procedure is illustrated in Figure 2a.

2.2.3. Path planning

After slicing is completed, infill paths within each layer must be further generated. Infill paths directly determine material distribution, pore structure, mechanical anisotropy, and nutrient diffusion behavior, making them important factors affecting the quality of tissue regeneration in *in situ* printing. Common path patterns include parallel grids, cross grids, and biomimetic gradient paths.[35] Parallel and cross-grid paths are widely adopted because of their simple implementation and high controllability, making these two grid structures the mainstream approaches in current applications. Biomimetic gradient paths were developed to address the complex gradient heterogeneity exhibited by native osteochondral units. Scaffolds fabricated using such paths possess smooth interlayer gradient transitions, which can significantly reduce the occurrence of complex problems such as scaffold delamination.[36]

In *in situ* bioprinting, infill path planning must additionally consider nozzle pose constraints, tissue curvature variations, and local accessibility. Especially in robotic-arm or minimally invasive printing systems, path planning often needs to be coupled with inverse kinematic analysis to avoid nozzle–tissue collisions, singular poses, and unreachable regions, thereby ensuring that the trajectories can be executed safely in real surgical environments. To address this issue, Zhao *et al.*[37] proposed a conformal algorithm that searches for optimal path points on point-cloud-approximated surfaces through constrained optimization, ensuring a high degree of similarity in both shape and angle between the predefined planar paths and the mapped 3D surface paths. They further designed multilayer conformal paths on a mouse dorsal wound model and used a self-developed multi-degree-of-freedom bioprinter to perform wound filling.

2.2.4. Parameter mapping and trajectory correction

In situ bioprinting paths are not merely spatial geometric trajectories, but must be further mapped into executable process parameters, including nozzle speed, extrusion rate, and nozzle pose. On complex tissue surfaces, deposition quality is highly dependent on the dynamic matching relationship between nozzle speed and extrusion rate. If the nozzle speed is too high while the material supply is insufficient, filament breakage is likely to occur; conversely, excessive material supply may lead to accumulation or collapse.

For open-loop *in situ* printing systems, path planning is a one-time offline result. The entire system generally adopts a fixed set of printing parameters throughout the printing process. Therefore, before each printing task, researchers typically conduct experiments to determine the optimal printing parameters for the bioink.

For closed-loop *in situ* printing systems, path planning is no longer a one-time offline result, but instead becomes a dynamically updatable online process. During execution, the system continuously receives sensor feedback and performs real-time replanning of local trajectories, including nozzle height compensation and local path offset correction. The work conducted by Kucukdeger and Johnson,[27] as mentioned earlier, is an example of this approach.

The correction of printing parameters can be achieved based on the detection results of hydrogel printing defects. Jin et al.38 developed an anomaly detection system based on layer-by-layer sensor images and machine learning algorithms. This system is capable of detecting and localizing discontinuity, irregularity, and non-uniformity defects, showing the potential for real-time autonomous correction of printing process parameters. The correction process is as follows: first, the system evaluates parameters such as the line width and continuity of the hydrogel. If defects are detected, the printing parameters are corrected accordingly. Since G-code contains part of the printing parameter information, the correction of printing parameters here essentially refers to modifying the parameters within the G-code. For parameters that are not included in the G-code, such as the air pressure parameter in extrusion-based printing, additional control of the pneumatic valve is required. Figure 2b shows the detection and positioning of hydrogel defects.

3. Application scenarios and bioinks

In *in situ* bioprinting, specific application scenarios determine the final choice of printing strategies, device configurations, and material systems.[39] Here, based on the mode of intervention and the manner in which the tissue printing environment is integrated, application scenarios are classified into three categories: body-surface and open-exposure scenarios, minimally invasive intervention scenarios, and remotely energy-driven scenarios. In addition, a biosensing scenario is introduced as an extended application direction.

The material system mainly involves the selection of bioinks, which largely affects multiple variables associated with *in situ* bioprinting, including cell viability, biocompatibility, and the mechanical properties of the printed constructs.[40-42] Researchers can improve the properties of bioinks by adjusting their compositions to

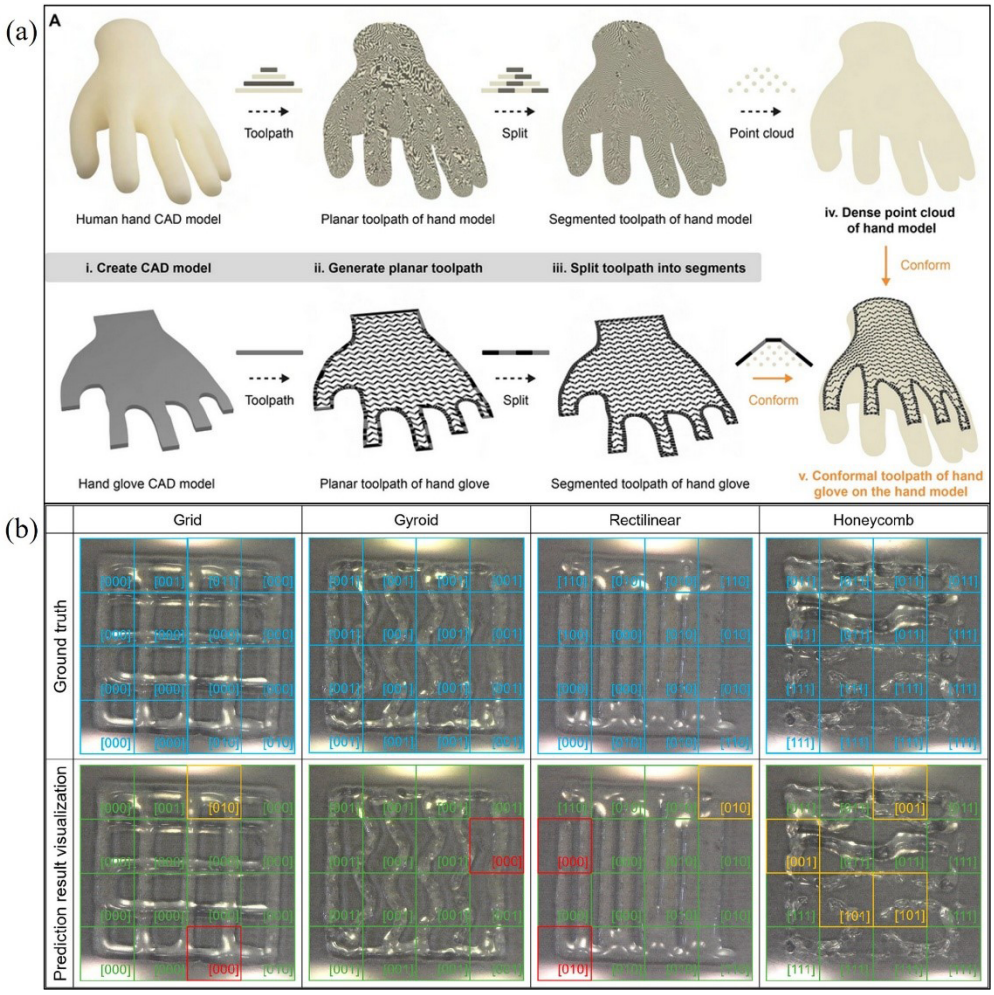

Figure 2. Schematic of the conformal algorithm and hydrogel defect identification. (a) Schematic diagram of the conformal algorithm proposed by Ji *et al.*,[34] which adopts a point cloud matching method. With this strategy, the system is not required to calculate the intersection position between the substrate and the target printing region. Instead, it only needs to slice the two parts separately and perform height compensation for each point of the target printing area. Reprinted from Ji *et al.*;[34] (b) Detection results of hydrogel defects. The system can not only classify three types of defects but also realize defect localization. Reprinted with permission from Jin *et al.*[38] Copyright © 2023 ACS Biomater. Sci. Eng.

accommodate specific application scenarios.

3.1. Body-surface and open-exposure scenarios

These environments are commonly encountered in skin repair as well as in the repair of superficial tissues such as bone and cartilage. These scenarios share several characteristics, including sufficient exposure of the target region, favorable visualization conditions, and ample operational space. As a result, they can provide relatively high positioning accuracy and operational flexibility for *in situ* bioprinting, making them one of the most mature and thoroughly validated application directions in current *in situ* bioprinting research.

In bone and osteochondral repair scenarios, bioinks must first satisfy relatively high mechanical requirements. Unlike soft tissues such as skin, bone defect regions are subjected to long-term compressive, shear, and locally concentrated stress environments during the repair process. Therefore, printed structures must not only exhibit good printability but also provide sufficient initial support capacity after fabrication to maintain the spatial stability of the defect region and withstand early physiological loads. To this end, bioinks for *in situ* bone repair are typically based on natural polymers and are further combined with bioceramics, nanoparticles, or mineralizable components to enhance the modulus, compressive strength, and osteogenic induction capability of the system.[43-45] Hindi *et al.*[46] adopted this strategy by combining alginate with hydroxyapatite, thereby balancing extrusion stability, structural support capability, and mimicry of the

osteogenic microenvironment, and successfully completed bone defect repair on rabbit calvaria. Figure 3a illustrates the repair process.

In addition to mechanical properties, cell adhesion is also a factor that needs to be considered. Particularly in relatively thick bone repair structures, if effective nutrient exchange channels are absent within the interior, cell survival and subsequent osteogenic efficiency will be significantly limited. One feasible approach is to improve the internal mass transfer environment by constructing predefined pores or transformable microchannels, thereby enabling the scaffold to maintain overall structural stability while providing enhanced permeability for nutrient transport and cell migration. The work of Shen *et al.*[47] reflects this concept. They used four-dimensional (4D) materials as cell carriers and incorporated polylactic acid (PLA)-polyethylene glycol (PEG)-PLA (3P) into hydrogel-based bioinks to form hollow channels that allow cells to distribute uniformly. During printing, 3P enabled endothelial cells to be evenly distributed, and after printing, it could transform into a gel state under temperature control and remain directly on the inner walls of the channels, forming a vessel-like endothelial

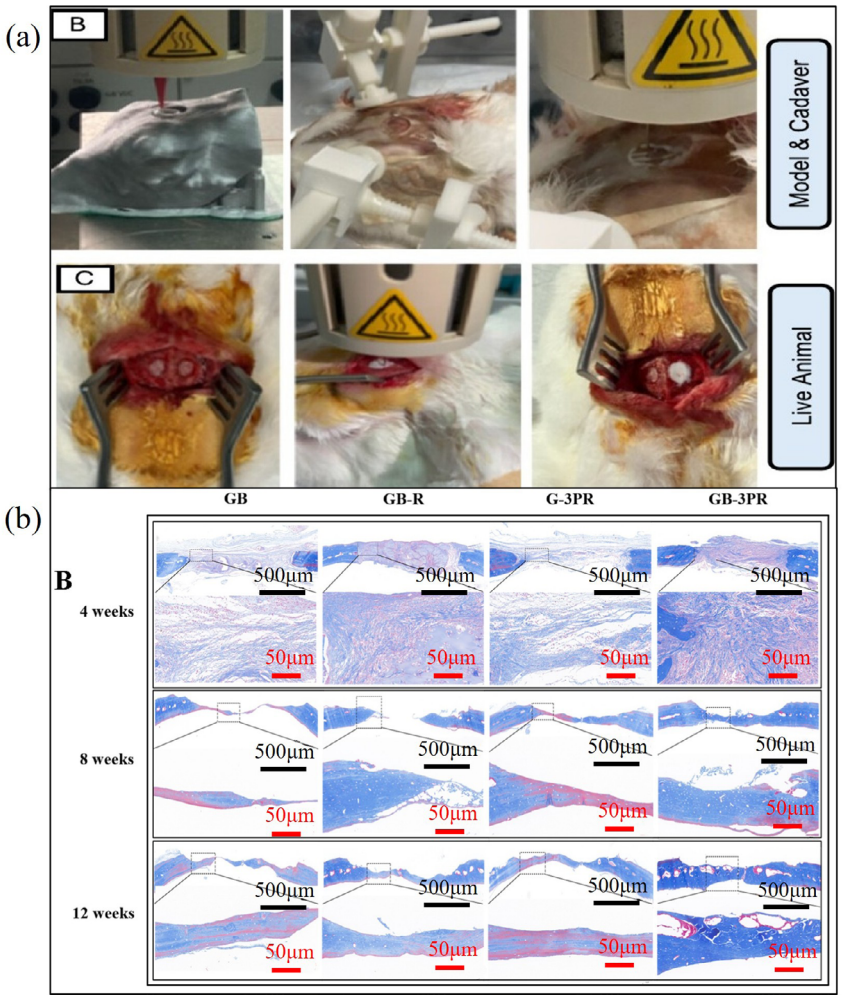

Figure 3. Bone repair applied to the body surface and open exposure scenarios. (a) Workflow of rabbit skull repair. Before animal experiments, the research team optimized the bioprinting procedure using a 3D-printed rabbit head model. Reprinted from Hindi *et al.*[46] (b) Histological staining images showing bone repair outcomes. The GB-3PR group, comprising 3D dual-extrusion bioprinted BMSC-laden GelMA hydrogel and RAOEC-laden 3P hydrogel scaffolds, showed the most complete bone repair by week 8 and exhibited the most favorable healing outcome. Reprinted with permission from Shen *et al.*[47] Copyright © 2022 The Authors. Published by Elsevier Ltd.

Abbreviations: BMSC: Bone mesenchymal stem cell; GB: 3D-bioprinted BMSC-laden GelMA hydrogel scaffold; GB-3PR: 3D dual-extrusion bioprinted BMSC-laden GelMA hydrogel and RAOEC-laden 3P hydrogel scaffold; GB-R: 3D-bioprinted BMSC-laden GelMA hydrogel scaffold with RAOECs; G-3PR: 3D dual-extrusion bioprinted GelMA hydrogel and RAOEC-laden 3P hydrogel scaffold; GelMA: Gelatin methacryloyl; RAOEC: Rat aortic endothelial cell.

layer. Results from rat calvarial defect repair experiments demonstrated that this scaffold could promote new bone formation in critical-sized rat calvarial defects. Figure 3b displays the repair results for each group.

Because skin wounds usually have irregular, moist surfaces and are subject to some degree of stretching, bioinks should exhibit strong adhesiveness and elasticity. Researchers can regulate the adhesiveness and elasticity of bioinks by adjusting the concentration of natural components or incorporating inorganic materials.[48,49] The work by Wang *et al.*[50] adopted this approach. They developed two types of bioinks by introducing different materials into the matrix: one was an Laponite XLG-based bioink derived from synthetic lithium saponite, which exhibited relatively high viscosity and could also construct high-strength scaffolds; the other was a low-viscosity granular hydrogel bioink based on hyaluronic acid and PEGDA, which additionally possessed softness and flexibility. They subsequently performed *in vitro* porcine skin wound repair and *in vivo* rat full-thickness skin wound repair experiments, and the results shown in Figure 4a reveal that the bioinks could effectively seal and uniformly cover the wounds.

Merely achieving wound coverage often provides only a temporary physical barrier and is insufficient to adequately promote wound healing and tissue reconstruction. One possible strategy is to use animal tissue-derived components as materials for hydrogel matrices.[51,52] Albanna *et al.*[53] incorporated autologous dermal fibroblasts and epidermal keratinocytes into bioinks and used these bioinks to perform repair in a porcine large-area full-thickness skin defect model. As shown in Figure 4b, the results demonstrated that, compared with the acellular matrix group, the allogeneic cell group, and the untreated group, the autologous cell *in situ* printing group exhibited a faster wound closure rate, lower contraction rate, and higher re-epithelialization efficiency. Specifically, wound closure occurred approximately three weeks earlier than in the control groups, while the re-epithelialization process was accelerated by approximately four to five weeks. In addition, the repaired tissue formed dermal structures, collagen arrangements, and mature vascular networks more closely resembling those of natural skin, demonstrating favorable tissue reconstruction capability.

3.2. Minimally invasive intervention scenarios

The scenarios discussed above generally require sufficient exposure of the target tissue during surgery; otherwise, a large incision must be created on the surface of the organism to fully expose the target tissue to the external environment. This provides sufficient spatial adaptability and operational flexibility for bioprinting procedures, but it remains inadequate in terms of precise manipulation and safe access within spatially constrained surgical environments. Integrating *in situ* bioprinting with minimally invasive surgery is a feasible approach.

Organ repair has always been a major research focus in *in situ* bioprinting. Compared with tissues such as skin, bone, and cartilage, organ surfaces are more complex, and immune rejection responses are more severe. Therefore, organ repair imposes higher requirements on the structural complexity, biological functionality, and microenvironmental adaptability of *in situ* bioprinting.[54] Such application scenarios drive the design of bioinks toward enhanced biocompatibility and elasticity, while also demanding higher precision from the actuators.

The microstructure of the liver is highly complex, which means that bioinks or printing conditions that generate high shear forces may compromise cell viability and tissue compatibility and are therefore less suitable for liver repair. To address this limitation, Zhao *et al.*[31] incorporated poly (acrylic acid)-N-hydroxysuccinimide ester into a hydrogel matrix to enhance tissue adhesiveness of the bioink, and used a seven-axis robot based on trocar needle recognition to perform liver repair in liver tissue, achieving favorable printing results and minimal contact force control at the incision site. The repair process is shown in Figure 5a.

To address the problem of premature rupture of fetal membranes, Zhao *et al.*[55] further developed an ultrafast light-responsive hydrogel, GMPD, in which PEGDA serves to delay thermal degradation of the hydrogel. The printing device was mounted at the end of a seven-degree-of-freedom robotic arm and served as a minimally invasive surgical actuator. Using this printing system, the team successfully fabricated hydrogel patches with gel rivet structures underwater. These patches exhibited strong tissue adhesion, good biocompatibility, mechanical properties similar to natural tissue, and appropriate sealing duration, effectively extending the gestation period.

Flexible bioprinting platforms are also a type of printing platform developed within the context of minimally invasive surgical applications. Such platforms can access target printing regions through minimally invasive incisions or natural orifices, offering a wide workspace and relatively high printing precision. Thai *et al.*[56] integrated a highly flexible soft printing head into a flexible robotic arm and designed a multifunctional flexible *in situ* 3D bioprinter, which is capable of printing biomaterials on fresh porcine kidneys and artificial colons. The repair process is shown in Figure 5b.

In situ bioprinting combined with minimally

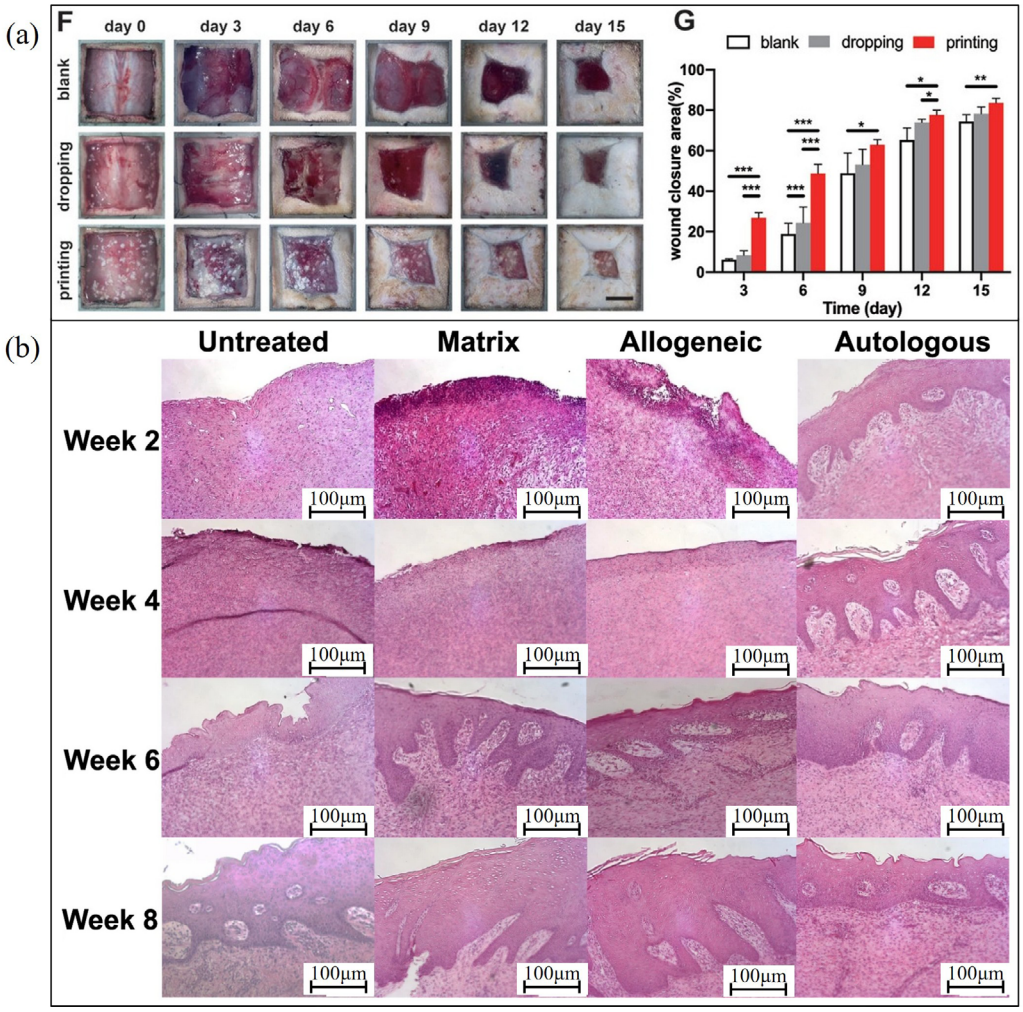

Figure 4. Skin repair applied to the body surface and open exposure scenarios. (a) Compared with the blank group and the drop printing group, the group treated with the handheld *in situ* bioprinter exhibited the fastest recovery rate and the best healing effect, and the highest level of wound protection was also observed. Reprinted from Wang *et al.*;[50] (b) Staining results of wound healing. Wounds treated with bioprinted autologous cells achieved faster and superior healing outcomes, demonstrating that the incorporation of autologous skin cells into hydrogel matrices can accelerate wound repair. Reprinted from Albanna *et al.*[53]

invasive surgery is not limited to changing the form of the robotic arm end effector; the use of alternative driving methods is also a feasible approach. Zhou *et al.*[57] designed a magnetically driven computer-controlled minimally invasive *in situ* bioprinting system known as the ferromagnetic soft catheter robot (FSCR) system. This system uses a set of computer-controlled motors to generate controllable magnetic fields, enabling printing on the surface of rat livers. The repair process is shown in Figure 5c. However, the FSCR relied on CT-based preoperative reconstruction. Therefore, unpredictable collisions could occur intraoperatively due to dynamic organ movement, thereby affecting printing quality. To address this, Hu *et al.*[58] developed a binocular vision-assisted magnetic soft catheter robotic system, which completed the *in situ* bioprinting process for a cartilage defect in 88 seconds.

3.3. Remotely energy-driven scenarios

Acoustic printing is an *in situ* manufacturing strategy that uses acoustic fields to remotely regulate the formation of biomaterials. Its basic principle is to convert acoustic energy into localized controllable physical or chemical stimuli through focused ultrasound, cavitation effects, or acoustofluidic induction, thereby triggering localized crosslinking, polymerization, or cellular assembly of bioinks in the target region, ultimately achieving *in situ* construction of structures.[59,60] Because this process does not require a rigid nozzle to directly contact the tissue

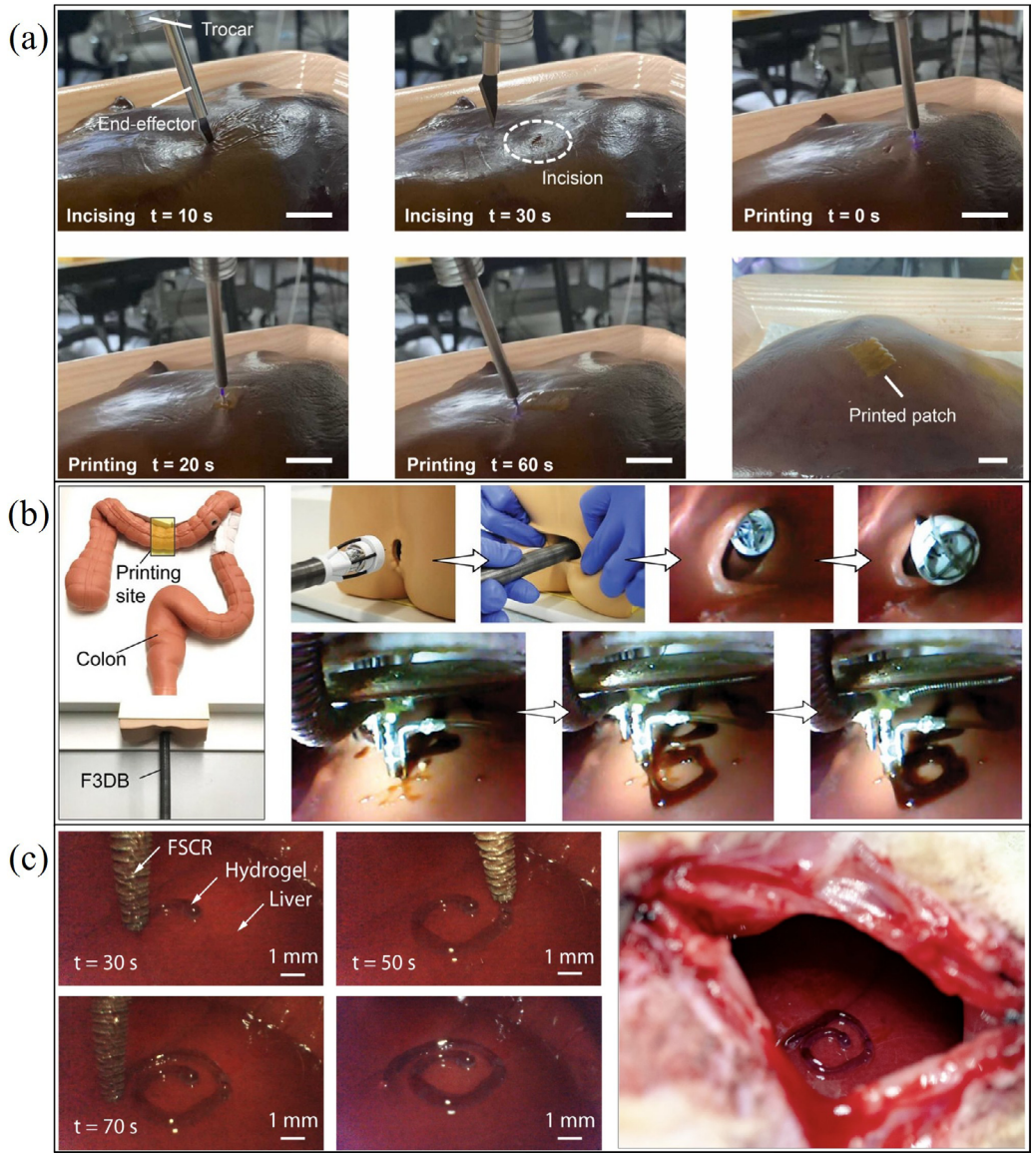

Figure 5. Repair of internal organs via minimally invasive surgery. (a) In the repair printing process on porcine liver, the hydrogel film adheres well to the tissue surface. Reprinted with permission from Zhao *et al.*[31] Copyright © 2023 Elsevier Inc. (b) *In situ* 3D bioprinter (F3DB) successfully performs endoscopic procedures in a simulated intestinal environment. Reprinted from Thai *et al.*[56] (c) Minimally invasive bioprinting on rat liver using ferromagnetic soft catheter robot (FSCR). Reprinted from Zhou *et al.*[57]

surface, acoustic printing can be considered a non-contact, low-mechanical-disturbance, remotely energy-driven mode of *in situ* printing. During the acoustic printing process, the system only needs to deliver the bioink into the body via a catheter or injection prior to printing. Once the bioink reaches the target printing region, an external actuator remotely induces crosslinking of the material at the body surface, thereby forming the desired structure.

Acoustic printing platforms, as a new paradigm of *in situ* bioprinting, represent a remotely energy-driven *in situ* bioprinting approach. Habibi *et al.*[61] developed the DSP platform, and Derayatifar *et al.*[62] subsequently developed the holographic DSP (HDSP) platform. The concept of the DSP platform originated from their sonochemiluminescence experiments using an alkaline aqueous solution of luminol (3-aminophthalhydrazide). They found that exploiting this reactivity in local regions of printed polymers could drive polymerization in those areas, thereby enabling material solidification. Based on

this property, Habibi *et al.*[61] developed the DSP platform, which may be regarded as the first-generation direct acoustic bioprinting platform. Figure 6a presents printing results on tissue phantoms. This platform consists of a transducer and a robotic arm. The printing performance can be improved by adjusting parameters such as the transducer driving pulse characteristics, the material, and the transducer configuration. However, the DSP printing region is limited to a single acoustic focal point, requiring voxel-by-voxel printing. To overcome this limitation, Derayatifar *et al.*[62] subsequently developed the HDSP platform as a second-generation direct acoustic bioprinting platform. This platform stores cross-sectional images of the desired components via acoustic holography, induces localized cavitation bubbles using wave-patterned acoustic fields, enabling on-demand regional polymerization as needed. This approach not only improves printing speed but also can yield layerless printed structures. The above studies mainly represent early conceptual validation of acoustic printing platforms and have not yet progressed to *in vivo* animal experimental validation. In the field of deep tissue *in situ* bioprinting, Davoodi *et al.*[63] developed a deep-tissue *in vivo* image-guided sound printing platform. They integrated gas vesicle ultrasound imaging into the printing system to achieve real-time monitoring of the printing process, precise focal localization, and verification of *in situ* crosslinking. They also performed *in vivo* printing in the bladder and muscles of live animals. The study demonstrated that acoustic printing not only enables remote patterning within deep tissues but also has the potential to be coupled with imaging systems, laying the foundation for closed-loop acoustic printing.

Sun *et al.*[64] further proposed a reconfigurable acoustic printing strategy, extending acoustic printing toward remote repair and structural reconstruction. This platform uses focused ultrasound waves to drive bioacoustic inks for solidification under centimeter-scale tissue penetration, and further induces localized softening and controllable deformation of materials through acoustic stimulation. Experiments were conducted on skull repair in live rabbits and cranial defect repair in dogs. The two *in vivo* validation studies demonstrated that acoustic printing can not only serve as a remote *in situ* fabrication approach, but can also be combined with minimally invasive repair to achieve reconfigurable fabrication of deep tissues. Figure 6b displays outcomes of canine skull defect repair.

Wu *et al.*[65] also developed an acoustic bioprinting platform. The team proposed an ultrahigh cell density (UHCD) bioprinting platform based on acoustic fluid-mediated stereolithography (ASL) technology. The ASL technique induces vortices through focused surface acoustic waves, causing cell aggregation at pre-polymerized solid–liquid interfaces, enabling the bioprinting of arbitrary multicellular structures. Figure 6c shows the UHCD bioprinting platform and related printing results on rabbit livers.

3.4. Biosensing

Although *in situ* bioprinting is primarily aimed at tissue repair and regeneration, its ability to directly deposit functional materials on the surface of living tissues also gives it another important application potential: the *in situ* construction of biosensing interfaces. In this scenario, *in situ* bioprinting is no longer limited to structural reconstruction of damaged tissues, but can directly fabricate flexible, conformal, and functional bioelectronic devices on biological tissue surfaces for physiological monitoring and therapeutic feedback.[66]

This application direction remains closely aligned with the core concept of *in situ* bioprinting, as it similarly relies on direct deposition on dynamic and irregular biological surfaces, adaptive matching to target geometries, and the stable fabrication of functional materials under physiological conditions. *In situ* bioprinting enables the direct construction of freeform functional devices conforming to target tissue surfaces. This, in turn, extends the application boundary of *in situ* bioprinting from structural repair to remote operation, medical treatment, and health monitoring.[67]

In such applications, bioinks must not only exhibit good printability and biocompatibility, but also prioritize stretchability, electrical conductivity, and stable signal transmission under dynamic deformation conditions, in order to adapt to the continuous deformation of biological tissue surfaces and the requirements of functional monitoring. Zhu *et al.*[28] proposed a method called "adaptive 3D bioprinting." They emphasized that the key to this process lies in developing functional bioinks that meet both conductivity and processability under natural conditions. They ultimately developed a bioink composed of polyethylene oxide as the matrix and silver flakes as the conductive filler. Using a closed-loop printing system integrated with a structured-light scanner, they fabricated wirelessly powered devices and wireless humidity sensors on moving human hands, and autonomously deposited cell-laden hydrogels at target locations in live mice. The results are shown in Figure 7a.

Electrical impedance tomography is a medical imaging technique that forms images of the body using electrical currents.[68,69] Due to its high temporal resolution, portability, and lack of ionizing radiation, EIT is suitable for biosensing applications.[70] Clinically, it has been applied

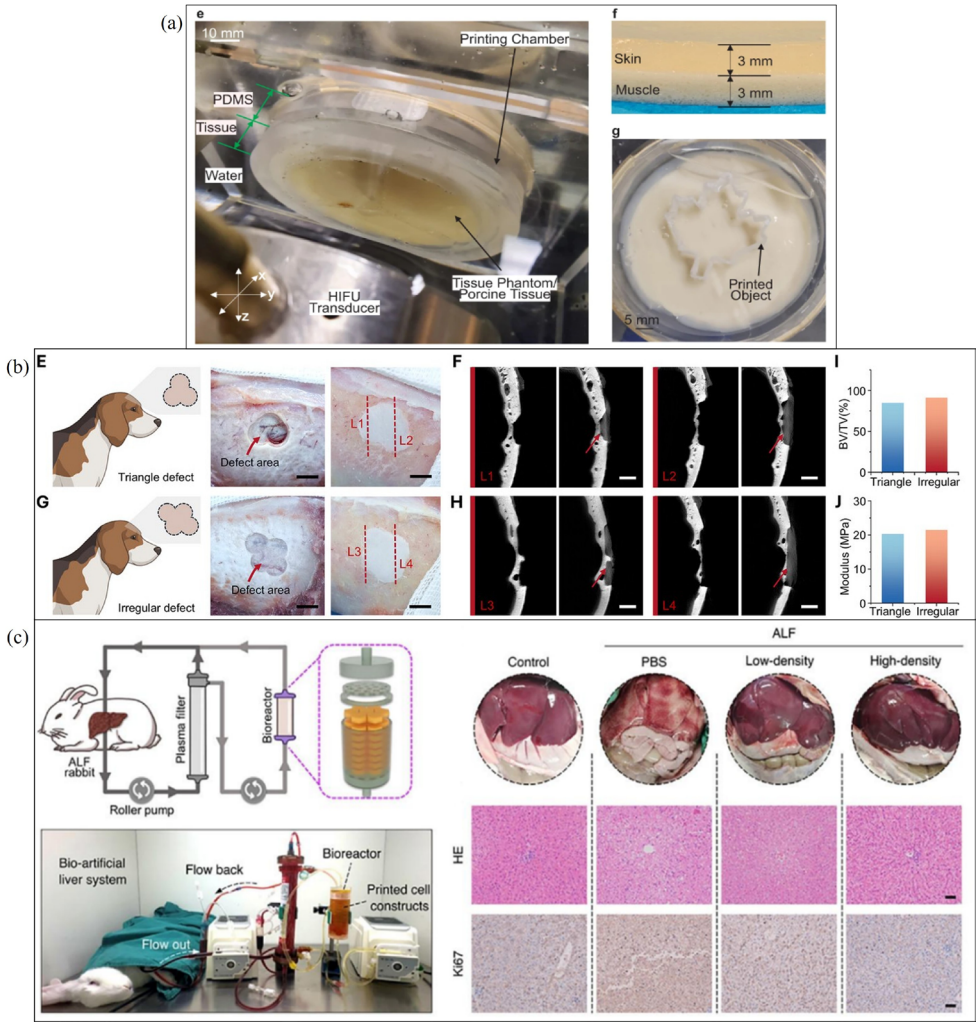

Figure 6. Concepts and biological experiments of acoustic printing. (a) External ear tissue was fabricated via the direct sound printing platform, and the fabrication was completed under simulated skin. Although no *in vivo* animal verification was performed, this work provides valuable insights and references for subsequent biological printing of auricular tissues. Reprinted from Habibi *et al.*[61] (b) Canine cranial defect repair results. Both triangular and irregular defects were fully filled; the printed repair materials exhibited favorable mechanical properties. Reprinted with permission from Sun *et al.*,[64] Copyright © 2026 Wiley-VCH GmbH. (c) Bioprinting results on rabbit liver using the ultrahigh cell density platform. The liver condition of rabbits with ALF was significantly improved after treatment. Reprinted with permission from Wu *et al.*[65] Copyright © 2025 Wiley-VCH GmbH.
Abbreviations: ALF: Acute liver failure; BV/TV: Bone volume/total volume; HE: Hematoxylin and eosin; HIFU: High-intensity focused ultrasound; Ki-67: Marker of proliferation Ki-67; PBS: Phosphate-buffered saline; PDMS: Polydimethylsiloxane.

to guide care for patients with acute respiratory distress syndrome.[71] In a related study, Zhu *et al.*[29] investigated 3D-printed wearable sensors combining ionic hydrogels with EIT technology using a closed-loop printing system composed of a stereo camera system and a structured-light 3D scanner. The team developed an ionic hydrogel with polyacrylamide as the matrix and LiCl as the ionic conductive medium, and directly fabricated EIT strain sensors on the surface of pig lungs undergoing respiration-induced deformation. The printing results are shown in Figure 7b. These sensors not only monitored *in situ* lung deformation but also maintained close adhesion to the lung surface under repeated deformation.

3.5. Bioink materials and design considerations

In *in situ* bioprinting systems, bioinks not only serve the roles of carrying cells, delivering bioactive factors, and constructing the microenvironment for new tissue formation, but also need to maintain good printability, biocompatibility, and adaptability in complex, dynamic, and often traumatically affected *in vivo* environments.[72,73] A wide range of materials has already been applied in the

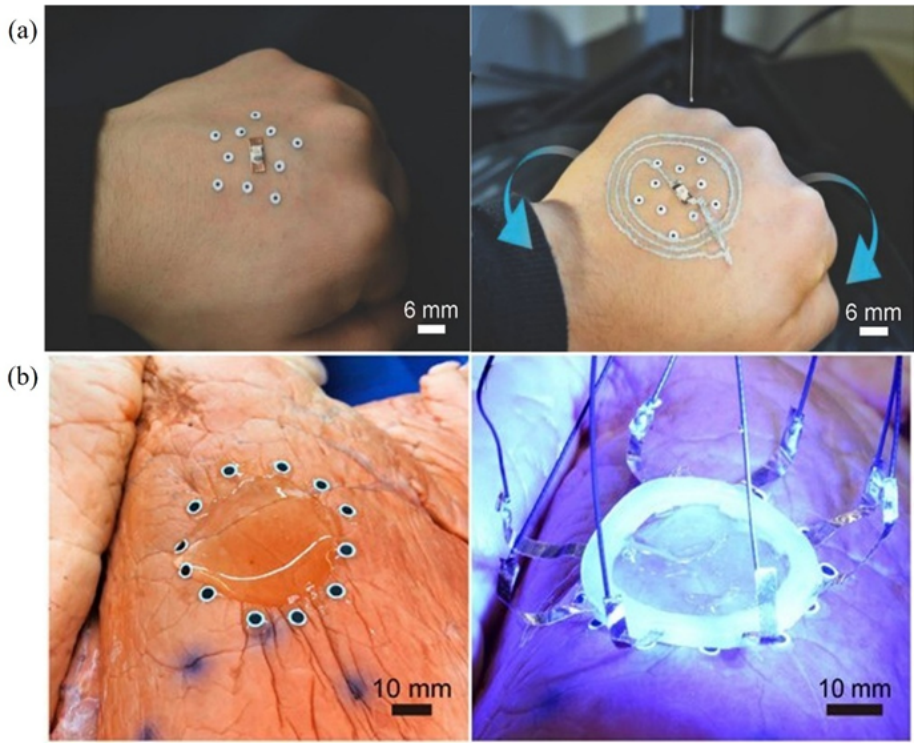

Figure 7. *In situ* bioprinting of electrical impedance tomography sensors on living tissue surfaces. (a) Multifunctional devices were fabricated on moving human hands, in which hydrogel lines served as conductive components. This printing system was also applied to the repair of skin defects on the dorsum of mice. Reprinted with permission from Zhu *et al.*[28] Copyright © 2018 WILEY-VCH Verlag GmbH & Co. KGaA, Weinheim. (b) *In situ* fabrication results on deformed porcine lungs. The average printing error was 0.657 mm, and the sensor could monitor lung deformation under external stimulation. Reprinted with permission from Zhu *et al.*[29] Copyright © 2020, The American Association for the Advancement of Science.

fabrication of bioinks. According to the classifications by Bramhe *et al.*[74] and Kim *et al.*,[75] materials used in bioinks can be divided into natural polymers and synthetic polymers: common natural polymers include collagen, chitosan, alginate, gelatin methacryloyl, fibrinogen, hyaluronic acid, cellulose, agarose, and carrageenan; while commonly used synthetic polymers include poly(lactic-co-glycolic acid), polycaprolactone (PCL), PLA, PEG, polyethylene oxide, and polyacrylamide. Natural polymers generally exhibit excellent biocompatibility and are the most widely used materials in bioink formulations; however, their mechanical properties are relatively weak, making them suitable for applications such as skin repair, soft tissues, and blood vessels. In contrast, synthetic polymers can modulate mechanical properties but generally have low bioactivity; therefore, they are often blended with natural polymers to tune bioink performance. Composite bioinks are typically composed of natural polymers combined with synthetic polymers, bioceramics, or nanomaterials, and represent the current mainstream trend in bioink development.

An ideal bioink should possess excellent biocompatibility to ensure non-toxicity, non-inflammatory response, and support for cell survival and development. It should also exhibit appropriate printability to ensure stable extrusion, high structural fidelity, and suitable viscosity. In addition, bioinks should have functions such as rapid crosslinking, fast and non-toxic degradation, strong tissue adhesiveness, and promotion of tissue regeneration.

Most currently used bioinks rely on photocuring or gelation processes to convert biological materials from a liquid state into a gel-like structure, which adheres to tissue and forms single-layer or multilayer architectures.[76,77] Depending on the target tissue, the design, processing, and composition of bioinks vary. For example, LAP can be added to hydrogel matrices to accelerate curing and address hydrogel degradation issues;[78] gelatin can undergo electrochemical treatment to form bio-concrete bioinks with strong rheological properties for bone repair applications; bioconcrete can be incorporated into gelatin–alginate hydrogel matrices to increase ink viscosity and scaffold Young's modulus;[79] nanoparticles or oxides can be introduced into hydrogel matrices to enhance scaffold mechanical properties.[80,81] Further information concerning the materials used in bioinks can be found in Table 1.

Table 1. Natural polymers, synthetic polymers, and 4D materials with potential applications in *in situ* bioprinting

Category	Material	Properties	Application Scenarios	Ref
Natural polymers	Collagen	Good cell adhesion and biocompatibility, but low mechanical strength and slow gelation rate	Skin repair, cartilage repair	[82]
	Gelatin/GelMA	Good cell affinity and modifiability; GelMA in particular possesses both natural bioactivity and photocrosslinking ability	Skin wounds, muscle injury, cartilage repair, and flexible biosensor substrates	[83]
	Alginate	Good printability, fast crosslinking with Ca^{2+}, but poor cell adhesion	Usually used in combination with other materials	[25]
	HA	High water retention and excellent lubricity	Cartilage repair, skin filling, and soft tissue regeneration	[84]
	Fibrin / Fibrinogen	Good tissue adhesion and hemostatic properties	Skin injury repair	[51]
	Chitosan	Natural antibacterial activity and favorable biocompatibility	Skin repair	[85]
	Cellulose[a]	Good rheological regulation capability	Commonly used as a rheological modifier or thickening support agent; also applicable for bone repair	[86]
	dECM	Provides a microenvironment close to natural tissues	Tissue repair such as muscle and cartilage	[52]
Synthetic polymers	PEG and its derivatives (PEGDA, 4-arm PEG)	Good biocompatibility, rapid curing, and stable structure	Bone repair, cartilage scaffolds, and minimally invasive organ surface sealing	[87]
	PAM	Elasticity and excellent stretchability	Flexible sensors	[29]
	PLA[a]	High mechanical strength and biodegradability	Bone repair	[57]
	PCL[a]	Excellent mechanical properties but slow degradation	Generally used in load-bearing scenarios such as bone support	[88]
	PLGA[a]	Tunable degradation rate	Used in scenarios requiring adjustable degradation rates	[89]
	Polyacrylic acids (PAA-NHS, etc.)	Good bioadhesion	Used for visceral tissue surface repair to enhance tissue adhesion	[90]
	PLATMC[a]	Biodegradable, good biocompatibility, tunable mechanical properties	Bone repair	[89]
	β-TCP[a]	Fast degradation rate and excellent biocompatibility	Bone repair	[89]
	PNIPAM[a]	Rapid and controllable deformation, good biocompatibility	Skin repair	[90]
	MNP[a]	Magnetic responsiveness	Cartilage repair; usually added to hydrogel matrices as a functional component	[91]
	Acrylate-based[a]	Fast curing rate, tunable mechanical properties	Gastric or intestinal inner wall repair	[92]

Notes: [a] indicates 4D materials. The applications of 4D materials are not directly for *in situ* bioprinting, but are potential uses or have been proven promising in *in situ* bioprinting under other contexts.

Abbreviations: β-TCP: β-tricalcium phosphate; dECM: Decellularized extracellular matrix; HA: Hyaluronic acid; MNP: Magnetic nanoparticles; PAA-NHS: Poly(acrylic acid)-N-hydroxysuccinimide ester; PAM: Polyacrylamide; PCL: poly-ε-caprolactone; PEG: Polyethylene glycol; PEGDA: Poly(ethylene glycol) diacrylate; PLA: Polylactic acid; PLGA: Poly(lactic-co-glycolic acid); PLA-TMC: Poly(L-lactide-co-trimethylene carbonate); PNIPAM: Poly(N-isopropyl acrylamide).

4. Conclusion and outlook

With the continuous integration of tissue engineering, biomanufacturing, and clinical regenerative medicine, *in situ* bioprinting is gradually transitioning from a laboratory concept to practical medical applications. Its core value lies in its ability to directly construct tissue structures at the site of injury, rapidly provide a cell-friendly microenvironment, and promote tissue repair in a highly personalized and minimally invasive manner.

From the perspective of technological development, control strategies are gradually transitioning from static path planning to dynamic environment-adaptive adjustments. In the future, tighter integration with multi-sensor fusion and autonomous control algorithms will be required to cope with complex wound geometries and highly dynamic *in vivo* conditions. In this process, AI technologies, particularly machine learning- and deep learning-based methods, are expected to play an important role in multimodal data fusion, real-time state recognition, and dynamic path optimization, thereby improving both the efficiency and precision of printing. As application scenarios expand from body surfaces to deep organs, existing systems still face challenges in positioning accuracy, response speed, and robustness in complex environments. These issues become even more pronounced during the transition from animal models to human applications. In this context, integrating AI may be a feasible approach, and some studies have already explored its potential.[93-95] For example, Zhu *et al.*[31] noted that AI can facilitate the execution, management, and coordination of *in situ* bioprinting workflows. As mentioned earlier, they also employed machine learning algorithms to learn a linear shape basis model of surface deformation. In addition, AI can be integrated with medical imaging technologies to achieve the integration of preoperative planning and intraoperative navigation, providing decision support for *in situ* printing in complex internal organs. There have already been some applications focusing on preoperative planning; for example, Li *et al.*[25] used AI to reconstruct a bone defect model before surgery. With the assistance of AI, combined with high-performance sensors, it may be possible to further advance the development of *in vivo* bioprinting. *In situ* bioprinting is gradually transitioning from an application stage focused on superficial tissue repair toward the repair of complex internal organs. At present, its applications in superficial or relatively stable tissues such as skin wounds and musculoskeletal injuries have undergone extensive experimental validation and are approaching early clinical investigation. These tissues offer good accessibility and visualization conditions, enabling high-precision deposition and real-time control. In contrast, for organs such as the liver and gastrointestinal tract, *in situ* bioprinting remains primarily at the stage of laboratory studies and animal model validation. For organ repair, with the assistance of flexible deployable printing tools, endoscopic platforms, and intraoperative navigation systems, *in situ* bioprinting is expected to achieve precise deposition in continuously moving or spatially constrained environments, thereby promoting its development toward minimally invasive or even intracavitary surgery. Recently, a research group has explored device localization issues by integrating two medical imaging modalities, CT and magnetic resonance imaging.[96] This may contribute to advances in visceral organ repair research.

Acoustic printing may also become a future research hotspot. Since Habibi *et al.*[61] developed the direct sound printing platform and Derayatifar *et al.*[62] subsequently developed holographic direct sound printing, many groups have explored acoustic printing with different materials and acoustic-field designs. Habibi *et al.*[61] also noted that one unique advantage of direct sound printing is its ability to print beyond optically opaque barriers, offering possibilities for non-invasive deep-tissue printing. However, acoustic printing is still in its early stages of development, and several key challenges remain for further applications. These include the significant impact of tissue heterogeneity on acoustic wave propagation and focusing accuracy in complex biological environments, the limited types of acoustically responsive bioinks, the unclear mechanisms by which cavitation behavior affects printing resolution and cell viability, and the lack of a stable closed-loop feedback system integrating real-time imaging, acoustic field regulation, and *in situ* crosslinking. Therefore, future development of acoustic printing will require further integration of medical imaging guidance, acoustic field control, acoustically responsive bioink design, and real-time closed-loop control strategies, in order to promote its transition from proof-of-concept studies toward a non-invasive *in situ* manufacturing platform for deep tissue applications.

Regarding bioinks, their physicochemical properties, curing mechanisms, and biological functions often determine whether *in situ* bioprinting can achieve the desired repair quality and clinical safety.[97,98] With the continuous evolution of actuator systems and fabrication strategies, higher demands are being placed on bioinks, including rapid gelation, injectability, multi-material synergistic printing, tunable mechanical properties, and the ability to promote tissue remodeling.[99,100] Some research groups have already explored the use of AI to assist in screening bioink properties and optimizing printing parameters, which also represents a potential application

of AI in *in situ* bioprinting.

In real physiological environments, *in situ* bioprinting often occurs on moist, warm tissue surfaces with physiological fluid flow; under such conditions, the gelation behavior, degradation rate, and mechanical matching of bioinks may change substantially.[101,102] Zhao *et al.*[103(p218)] pointed out: "Primarily in terms of the printing materials, i.e., bioinks, most efforts have focused on the modification and secondary development of existing bioinks used in conventional bioprinting, but there is always a trade-off between the various properties of bioinks required for *in vivo* bioprinting". Therefore, future studies need to further investigate the coupling mechanisms between material design and the real *in vivo* environment. According to the conclusions of Mirasadi *et al.*,[104] magnetically responsive shape memory polymers as 4D printing materials are expected to be extended to the field of *in situ* bioprinting. Such materials can be used to fabricate desired structures through magnetically driven control according to design. For example, in thermoplastic polymers such as PCL, the glass transition temperature is approximately −60°C and the melting temperature is around 60 °C, giving it high flexibility and biodegradability. By incorporating magnetically responsive Fe_3O_4 nanoparticles into PCL, an alternating magnetic field can be used to guide the bioink to aggregate at defect sites and form structures, providing mechanical support upon cooling and gradually degrading during tissue regeneration.[104-107] Therefore, Table 1 includes several 4D materials.

In real human physiological environments, complex physiological motions, multiscale mechanical coupling, and inter-individual variability exist, making the translation of animal experimental results into clinical practice still face significant challenges. *In situ* bioprinting also faces a series of regulatory and standardization challenges. Since it simultaneously involves biomaterials, living cells, and medical devices, its approval process must meet requirements related to biosafety, material controllability, and device reliability. In fact, some countries have already established relatively clear regulatory frameworks. For example, the United States considers bioprinted products as "combination products" consisting of drugs, biologics, and medical devices. In practice, most current regulatory frameworks are still based on this "combination product" concept, resulting in a patchwork-style regulatory approach rather than an independent regulatory system, although oversight is applied to each component product.

In addition, *in situ* bioprinting processes are highly dependent on real-time operating environments, and standards for process consistency, reproducibility, and quality control have not yet been fully established, which imposes higher demands on clinical safety evaluation. At the same time, the characteristics of personalized treatment make traditional evaluation systems difficult to directly apply; therefore, dynamic regulatory frameworks tailored to *in situ* manufacturing processes are still needed.

Acknowledgments

None.

Funding

This work was supported by the Frontier Technologies R&D Program of Jiangsu Province (Grant No. BF2024077) and Postgraduate Research & Practice Innovation Program of Jiangsu Province (SJCX25_0731).

Conflict of interest

Huixin Liang, Lan Li, and Qing Jiang serve as Editorial Board Members of this journal, but were not in any way involved in the editorial and peer-review process conducted for this paper, directly or indirectly. The authors declare no conflicts of interest.

Author contributions

Conceptualization: Zijun Zheng, Xinrong Tan, Huixin Liang
Supervision: Qing Jiang, Lan Li, Jianping Shi
Writing–original draft: Zijun Zheng
Writing–review & editing: Xinrong Tan

Ethics approval and consent to participate

Not applicable.

Consent for publication

Not applicable.

Availability of data

Not applicable.

References

1. Kumar MS, Varma P, Kandasubramanian B. From lab to life: advances in in-situ bioprinting and bioink technology. *Biomed Mater*. 2024;20(1):012004.

   doi: 10.1088/1748-605X/ad9dd0

2. Ng WL, Vyas C, Huang B, Yeong WY, Bartolo P. Advanced bioprinting strategies for fabrication of biomimetic tissues and organs. *Int J Extreme Manuf*. 2025;7(6):062006.

   doi: 10.1088/2631-7990/adeee0

3. Hu C, Wang C, Bian S, *et al*. In situ bioprinting: tailored printing strategies for regenerative medicine. *Int J Bioprint*. 2024;10(5):3366.

doi: 10.36922/ijb.3366

4. Jain P, Kathuria H, Ramakrishna S, Parab S, Pandey MM, Dubey N. In situ bioprinting: process, bioinks, and applications. *ACS Appl Bio Mater*. 2024;7(12):7987-8007.

   doi: 10.1021/acsabm.3c01303

5. Li X, Liu B, Pei B, *et al*. Inkjet bioprinting of biomaterials. *Chem Rev*. 2020;120(19):10793-10833.

   doi: 10.1021/acs.chemrev.0c00008

6. Liu J, Xu C. Improving uniformity of cell distribution in post-inkjet-based bioprinting. *J Manuf Sci Eng*. 2023;146(1):14501.

   doi: 10.1115/1.4063134

7. Jin S, Jing Y, Lu H, *et al*. Photocrosslinkable hydrogel microparticle bioink for digital-light-processing 3D bioprinting. *Small Methods*. 2025;9(8):2500115.

   doi: 10.1002/smtd.202500115

8. Li W, Wang M, Ma H, Chapa-Villarreal FA, Lobo AO, Zhang YS. Stereolithography apparatus and digital light processing-based 3D bioprinting for tissue fabrication. *iScience*. 2023;26(2):106039.

   doi: 10.1016/j.isci.2023.106039

9. Nieto D, Jorge de Mora A, Kalogeropoulou M, Bhusal A, K. Miri A, Moroni L. Bottom-up and top-down VAT photopolymerization bioprinting for rapid fabrication of multi-material microtissues. *Int J Bioprint*. 2024;10(2):1017.

   doi: 10.36922/ijb.1017

10. Jiao T, Lian Q, Zhao T, Wang H, Li D. Preparation, mechanical and biological properties of inkjet printed alginate/gelatin hydrogel. *J Bionic Eng*. 2021;18(3):574-583.

    doi: 10.1007/s42235-021-0036-9

11. Herberg S, Kondrikova G, Periyasamy-Thandavan S, *et al*. Inkjet-based biopatterning of SDF-1β augments BMP-2-induced repair of critical size calvarial bone defects in mice. *Bone*. 2014;67:95-103.

    doi: 10.1016/j.bone.2014.07.007

12. Li Y, Zhang X, Zhang X, Zhang Y, Hou D. Recent progress of the vat photopolymerization technique in tissue engineering: a brief review of mechanisms, methods, materials, and applications. *Polymers*. 2023;15(19):3940.

    doi: 10.3390/polym15193940

13. Ng WL, Lee JM, Zhou M, *et al*. Vat polymerization-based bioprinting—process, materials, applications and regulatory challenges. *Biofabrication*. 2020;12(2):022001.

    doi: 10.1088/1758-5090/ab6034

14. Zandrini T, Florczak S, Levato R, Ovsianikov A. Breaking the resolution limits of 3D bioprinting: future opportunities and present challenges. *Trends Biotechnol*. 2023;41(5):604-614.

    doi: 10.1016/j.tibtech.2022.10.009

15. Dubey N, Ferreira JA, Daghrery A, *et al*. Highly tunable bioactive fiber-reinforced hydrogel for guided bone regeneration. *Acta Biomater*. 2020;113:164-176.

    doi: 10.1016/j.actbio.2020.06.011

16. Liu J, Miller K, Ma X, *et al*. Direct 3D bioprinting of cardiac micro-tissues mimicking native myocardium. *Biomaterials*. 2020;256:120204.

    doi: 10.1016/j.biomaterials.2020.120204

17. Erben A, Hörning M, Hartmann B, *et al*. Precision 3D-printed cell scaffolds mimicking native tissue composition and mechanics. *Adv Healthc Mater*. 2020;9(24):2000918.

    doi: 10.1002/adhm.202000918

18. Jain P, Kathuria H, Dubey N. Advances in 3D bioprinting of tissues/organs for regenerative medicine and in-vitro models. *Biomaterials*. 2022;287:121639.

    doi: 10.1016/j.biomaterials.2022.121639

19. Kong YL, Tamargo IA, Kim H, *et al*. 3D printed quantum dot light-emitting diodes. *Nano Lett*. 2014;14(12):7017-7023.

    doi: 10.1021/nl5033292

20. Johnson BN, Lancaster KZ, Zhen G, *et al*. 3D printed anatomical nerve regeneration pathways. *Adv Funct Mater*. 2015;25(39):6205-6217.

    doi: 10.1002/adfm.201501760

21. Bader C, Patrick WG, Kolb D, *et al*. Grown, printed, and biologically augmented: an additively manufactured microfluidic wearable, functionally templated for synthetic microbes. *3D Print Addit Manuf*. 2016;3(2):79-89.

    doi: 10.1089/3dp.2016.0027

22. Jiang Y, Islam MdN, He R, *et al*. Recent advances in 3D printed sensors: materials, design, and manufacturing. *Adv Mater Technol*. 2023;8(2):2200492.

    doi: 10.1002/admt.202200492

23. Zhu Z, Ng DWH, Park HS, McAlpine MC. 3D-printed multifunctional materials enabled by artificial-intelligence-assisted fabrication technologies. *Nat Rev Mater*. 2021;6(1):27-47.

    doi: 10.1038/s41578-020-00235-2

24. Cohen DL, Lipton JI, Bonassar LJ, Lipson H. Additive manufacturing for in situ repair of osteochondral defects. *Biofabrication*. 2010;2(3):035004.

    doi: 10.1088/1758-5082/2/3/035004

25. Li L, Shi J, Ma K, *et al*. Robotic in situ 3D bio-printing technology for repairing large segmental bone defects. *J Adv Res*. 2021;30:75-84.

    doi: 10.1016/j.jare.2020.11.011

26. O'Neill JJ, Johnson RA, Dockter RL, Kowalewski TM. 3D bioprinting directly onto moving human anatomy. In: *2017 IEEE/RSJ International Conference on Intelligent Robots and Systems (IROS)*. IEEE; 2017:934-940.

    doi: 10.1109/IROS.2017.8202257

27. Kucukdeger E, Johnson BN. Closed-loop controlled conformal 3D printing on moving objects via tool-localized object position sensing. *J Manuf Processes*. 2023;89:39-49.

    doi: 10.1016/j.jmapro.2023.01.020

28. Zhu Z, Guo SZ, Hirdler T, *et al*. 3D printed functional and biological materials on moving freeform surfaces. *Adv Mater*. 2018;30(23):1707495.

    doi: 10.1002/adma.201707495

29. Zhu Z, Park HS, McAlpine MC. 3D printed deformable sensors. *Sci Adv*. 2020;6(25):eaba5575.

    doi: 10.1126/sciadv.aba5575

30. Derayatifar M, Habibi M, Bhat R, Packirisamy M. Penalization and deep learning algorithms in holographic direct sound printing to improve print uniformity. *Addit Manuf*. 2025;105:104782.

    doi: 10.1016/j.addma.2025.104782

31. Zhao W, Hu C, Lin S, *et al*. A closed-loop minimally invasive 3D printing strategy with robust trocar identification and adaptive alignment. *Addit Manuf*. 2023;73:103701.

    doi: 10.1016/j.addma.2023.103701

32. Fortunato GM, Sigismondi S, Nicoletta M, *et al*. Analysis of the robotic-based in situ bioprinting workflow for the regeneration of damaged tissues through a case study. *Bioengineering*. 2023;10(5):560.

    doi: 10.3390/bioengineering10050560

33. Alkadi F, Lee KC, Bashiri AH, Choi JW. Conformal additive manufacturing using a direct-print process. *Addit Manuf*. 2020;32:100975.

    doi: 10.1016/j.addma.2019.100975

34. Ji Z, Brion DAJ, Samson KDG, Pattinson SW. Facile method for 3D printing conformally onto uneven surfaces and its application to face masks. *Sci Rep*. 2023;13(1):21659.

    doi: 10.1038/s41598-023-48547-x

35. Chaudhry MS, Czekanski A. Surface slicing and toolpath planning for in-situ bioprinting of skin implants. *Biofabrication*. 2024;16(2):025030.

    doi: 10.1088/1758-5090/ad30c4

36. Lu J, Gao Y, Cao C, *et al*. 3D bioprinted scaffolds for osteochondral regeneration: Advancements and applications. *Mater Today Bio*. 2025;32:101834.

    doi: 10.1016/j.mtbio.2025.101834

37. Zhao W, Hu C, Wang Y, Lin S, Wang Z, Xu T. Optimization-based conformal path planning for in situ bioprinting during complex skin defect repair. *Bio-Des Manuf*. 2025;8(1):1-19.

    doi: 10.1631/bdm.2300365

38. Jin Z, Zhang Z, Shao X, Gu GX. Monitoring anomalies in 3D bioprinting with deep neural networks. *ACS Biomater Sci Eng*. 2023;9(7):3945-3952.

    doi: 10.1021/acsbiomaterials.0c01761

39. Clement N, Kandasubramanian B. 3D printed ionogels in sensors. *Polym-Plast Technol Mater*. 2023;62(5):632-654.

    doi: 10.1080/25740881.2022.2126784

40. Raees S, Ullah F, Javed F, *et al*. Classification, processing, and applications of bioink and 3D bioprinting: a detailed review. *Int J Biol Macromol*. 2023;232:123476.

    doi: 10.1016/j.ijbiomac.2023.123476

41. Wang Y, Kim HJ, Vunjak-Novakovic G, Kaplan DL. Stem cell-based tissue engineering with silk biomaterials. *Biomaterials*. 2006;27(36):6064-6082.

    doi: 10.1016/j.biomaterials.2006.07.008

42. Skardal A, Devarasetty M, Kang HW, *et al*. A hydrogel bioink toolkit for mimicking native tissue biochemical and mechanical properties in bioprinted tissue constructs. *Acta Biomater*. 2015;25:24-34.

    doi: 10.1016/j.actbio.2015.07.030

43. Xie M, Shi Y, Zhang C, *et al*. In situ 3D bioprinting with bioconcrete bioink. *Nat Commun*. 2022;13(1):3597.

    doi: 10.1038/s41467-022-30997-y

44. Chen G, Liang X, Zhang P, *et al*. Bioinspired 3D printing of functional materials by harnessing enzyme-induced biomineralization. *Adv Funct Mater*. 2022;32(34):2113262.

    doi: 10.1002/adfm.202113262

45. Xu C, Xia Y, Zhuang P, *et al*. FePSe3-nanosheets-integrated cryogenic-3D-printed multifunctional calcium phosphate scaffolds for synergistic therapy of osteosarcoma. *Small*. 2023;19(38):2303636.

    doi: 10.1002/smll.202303636

46. Hindi OA, Pinarbasi B, Bakici M, *et al*. In situ bioprinting enhances bone regeneration in a live animal model with craniofacial defect. *ACS Biomater Sci Eng*. 2025;11(8):5027-5037.

    doi: 10.1021/acsbiomaterials.5c00780

47. Shen M, Wang L, Gao Y, *et al*. 3D bioprinting of in situ vascularized tissue engineered bone for repairing large segmental bone defects. *Mater Today Bio*. 2022;16:100382.

    doi: 10.1016/j.mtbio.2022.100382

48. Quint JP, Mostafavi A, Endo Y, *et al*. In vivo printing of nanoenabled scaffolds for the treatment of skeletal muscle injuries. *Adv Healthc Mater*. 2021;10(10):2002152.

doi: 10.1002/adhm.202002152

49. Nuutila K, Samandari M, Endo Y, *et al*. In vivo printing of growth factor-eluting adhesive scaffolds improves wound healing. *Bioact Mater*. 2022;8:296-308.

doi: 10.1016/j.bioactmat.2021.06.030

50. Wang C, Hu C, Cheng H, *et al*. A programmable handheld extrusion-based bioprinting platform for in situ skin wounds dressing: balance mobility and customizability. *Adv Sci*. 2024;11(46):2405823.

doi: 10.1002/advs.202405823

51. Skardal A, Mack D, Kapetanovic E, *et al*. Bioprinted amniotic fluid-derived stem cells accelerate healing of large skin wounds. *Stem Cells Transl Med*. 2012;1(11):792-802.

doi: 10.5966/sctm.2012-0088

52. Choi YJ, Jun YJ, Kim DY, *et al*. A 3D cell printed muscle construct with tissue-derived bioink for the treatment of volumetric muscle loss. *Biomaterials*. 2019;206:160-169.

doi: 10.1016/j.biomaterials.2019.03.036

53. Albanna M, Binder KW, Murphy SV, *et al*. In situ bioprinting of autologous skin cells accelerates wound healing of extensive excisional full-thickness wounds. *Sci Rep*. 2019;9(1):1856.

doi: 10.1038/s41598-018-38366-w

54. Liu K, Yan L, Li R, *et al*. 3D printed personalized nerve guide conduits for precision repair of peripheral nerve defects. *Adv Sci*. 2022;9(12):2103875.

doi: 10.1002/advs.202103875

55. Zhao W, Hu C, Xu T, Lin S, Wang Z, Zhu Y. Subaqueous bioprinting: a novel strategy for fetal membrane repair with 7-axis robot-assisted minimally invasive surgery. *Adv Funct Mater*. 2022;32(51):2207496.

doi: 10.1002/adfm.202207496

56. Thai MT, Phan PT, Tran HA, *et al*. Advanced soft robotic system for in situ 3D bioprinting and endoscopic surgery. *Adv Sci*. 2023;10(12):2205656.

doi: 10.1002/advs.202205656

57. Zhou C, Yang Y, Wang J, *et al*. Ferromagnetic soft catheter robots for minimally invasive bioprinting. *Nat Commun*. 2021;12(1):5072.

doi: 10.1038/s41467-021-25386-w

58. Hu J, Guo L, Gu W, *et al*. Binocular vision-assisted magnetic soft catheter robot system for minimally invasive in-situ bioprinting. *IEEE Robot Autom Lett*. 2024;9(12):11130-11137.

doi: 10.1109/LRA.2024.3474552

59. Debbi L, Machour M, Dahis D, *et al*. Ultrasound mediated polymerization for cell delivery, drug delivery, and 3D printing. *Small Methods*. 2024;8(7):2301197.

doi: 10.1002/smtd.202301197

60. Ma Z, Holle AW, Melde K, *et al*. Acoustic holographic cell patterning in a biocompatible hydrogel. *Adv Mater*. 2020;32(4):1904181.

doi: 10.1002/adma.201904181

61. Habibi M, Foroughi S, Karamzadeh V, Packirisamy M. Direct sound printing. *Nat Commun*. 2022;13(1):1800.

doi: 10.1038/s41467-022-29395-1

62. Derayatifar M, Habibi M, Bhat R, Packirisamy M. Holographic direct sound printing. *Nat Commun*. 2024;15(1):6691.

doi: 10.1038/s41467-024-50923-8

63. Davoodi E, Li J, Ma X, *et al*. Imaging-guided deep tissue in vivo sound printing. *Science*. 2025;388(6747):616-623.

doi: 10.1126/science.adt0293

64. Sun C, Li Z, Osman A, *et al*. Reconfigurable acoustic printing for conformal and minimally invasive repair. *Adv Funct Mater*. 2026;36(26):e25723.

doi: 10.1002/adfm.202525723

65. Wu Z, Wang J, Huang D, Cheng Y, Zhao Y. Ultrahigh cell density 3D bioprinting by acoustic fluids-mediated stereolithography. *Adv Mater*. 2025;38(7):e11418.

doi: 10.1002/adma.202511418

66. Trampe E, Koren K, Akkineni AR, *et al*. Functionalized bioink with optical sensor nanoparticles for O2 imaging in 3D-bioprinted constructs. *Adv Funct Mater*. 2018;28(45):1804411.

doi: 10.1002/adfm.201804411

67. Gao Q, Lee JS, Kim BS, Gao G. Three-dimensional printing of smart constructs using stimuli-responsive biomaterials: A future direction of precision medicine. *Int J Bioprint*. 2022;9(1):638.

doi: 10.18063/ijb.v9i1.638

68. Creegan A, Ruddy B, Taberner A. A 3D phantom for EIT printed in a single part. *Med Eng Phys*. 2025;146(1):104428.

doi: 10.1016/j.medengphy.2025.104428

69. Silvera-Tawil D, Rye D, Soleimani M, Velonaki M. Electrical impedance tomography for artificial sensitive robotic skin: a review. *IEEE Sensors J*. 2015;15(4):2001-2016.

doi: 10.1109/JSEN.2014.2375346

70. Alawy A, Mostaghimi H, Amani S, Rezvani S, Park SS. Piezoresistive nanocomposite sensing using electrical impedance tomography and machine learning. *Sens Actuators A*. 2024;377:115778.

doi: 10.1016/j.sna.2024.115778

71. van der Zee P, Somhorst P, Endeman H, Gommers D. Electrical impedance tomography for positive end-

expiratory pressure titration in COVID-19–related acute respiratory distress syndrome. *Am J Respir Crit Care Med*. 2020;202(2):280-284.

doi: 10.1164/rccm.202003-0816LE

72. Fang W, Yang M, Wang L, *et al*. Hydrogels for 3D bioprinting in tissue engineering and regenerative medicine: current progress and challenges. *Int J Bioprint*. 2023;9(5):759.

doi: 10.18063/ijb.759

73. Advincula RC, Dizon JRC, Caldona EB, *et al*. On the progress of 3D-printed hydrogels for tissue engineering. *MRS Commun*. 2021;11(5):539-553.

doi: 10.1557/s43579-021-00069-1

74. Bramhe P, Rarokar N, Kumbhalkar R, Saoji S, Khedekar P. Natural and synthetic polymeric hydrogel: a bioink for 3D bioprinting of tissue models. *J Drug Delivery Sci Technol*. 2024;101:106204.

doi: 10.1016/j.jddst.2024.106204

75. Kim GJ, Kim L, Kwon OS. Application of 3D bioprinting technology for tissue regeneration, drug evaluation, and drug delivery. *Appl Sci Converg Technol*. 2023;32(1):1-6.

doi: 10.5757/ASCT.2023.32.1.1

76. Kim IL, Mauck RL, Burdick JA. Hydrogel design for cartilage tissue engineering: a case study with hyaluronic acid. *Biomaterials*. 2011;32(34):8771-8782.

doi: 10.1016/j.biomaterials.2011.08.073

77. Kesti M, Müller M, Becher J, *et al*. A versatile bioink for three-dimensional printing of cellular scaffolds based on thermally and photo-triggered tandem gelation. *Acta Biomater*. 2015;11:162-172.

doi: 10.1016/j.actbio.2014.09.033

78. Nguyen AK, Goering PL, Reipa V, Narayan RJ. Toxicity and photosensitizing assessment of gelatin methacryloyl-based hydrogels photoinitiated with lithium phenyl-2,4,6-trimethylbenzoylphosphinate in human primary renal proximal tubule epithelial cells. *Biointerphases*. 2019;14(2):021007.

doi: 10.1116/1.5095886

79. Sadeghian A, Kharaziha M, Khoroushi M. Dentin extracellular matrix loaded bioactive glass/GelMA support rapid bone mineralization for potential pulp regeneration. *Int J Biol Macromol*. 2023;234:123771.

doi: 10.1016/j.ijbiomac.2023.123771

80. Gao Q, Niu X, Shao L, *et al*. 3D printing of complex GelMA-based scaffolds with nanoclay. *Biofabrication*. 2019;11(3):035006.

doi: 10.1088/1758-5090/ab0cf6

81. Züger F, Marsano A, Poggio M, Gullo MR. Nanocomposites in 3D bioprinting for engineering conductive and stimuli-responsive constructs mimicking electrically sensitive tissue. *Adv NanoBiomed Res*. 2022;2(2):2100108.

doi: 10.1002/anbr.202100108

82. Levin AA, Karalkin PA, Koudan EV, *et al*. Commercial articulated collaborative in situ 3D bioprinter for skin wound healing. *Int J Bioprint*. 2023;9(2):675.

doi: 10.18063/ijb.v9i2.675

83. Di Bella C, Duchi S, O'Connell CD, *et al*. In situ handheld three-dimensional bioprinting for cartilage regeneration. *J Tissue Eng Regen Med*. 2018;12(3):611-621.

doi: 10.1002/term.2476

84. Ma K, Zhao T, Yang L, *et al*. Application of robotic-assisted in situ 3D printing in cartilage regeneration with HAMA hydrogel: an in vivo study. *J Adv Res*. 2020;23:123-132.

doi: 10.1016/j.jare.2020.01.010

85. Liu Y, Luo X, Wu W, *et al*. Dual cure (thermal/photo) composite hydrogel derived from chitosan/collagen for in situ 3D bioprinting. *Int J Biol Macromol*. 2021;182:689-700.

doi: 10.1016/j.ijbiomac.2021.04.058

86. Zhao H, Zhang Y, Liu Y, *et al*. In situ forming cellulose nanofibril-reinforced hyaluronic acid hydrogel for cartilage regeneration. *Biomacromolecules*. 2021;22(12):5097-5107.

doi: 10.1021/acs.biomac.1c01063

87. Xin S, Deo KA, Dai J, *et al*. Generalizing hydrogel microparticles into a new class of bioinks for extrusion bioprinting. *Sci Adv*. 2021;7(42):eabk3087.

doi: 10.1126/sciadv.abk3087

88. Liu X, Zhao K, Gong T, *et al*. Delivery of growth factors using a smart porous nanocomposite scaffold to repair a mandibular bone defect. *Biomacromolecules*. 2014;15(3):1019-1030.

doi: 10.1021/bm401911p

89. Wang C, Yue H, Liu J, *et al*. Advanced reconfigurable scaffolds fabricated by 4D printing for treating critical-size bone defects of irregular shapes. *Biofabrication*. 2020;12(4):045025.

doi: 10.1088/1758-5090/abab5b

90. Wang X, Yu Y, Yang C, Shang L, Zhao Y, Shen X. Dynamically responsive scaffolds from microfluidic 3D printing for skin flap regeneration. *Adv Sci*. 2022;9(22):2201155.

doi: 10.1002/advs.202201155

91. Chakraborty J, Fernández-Pérez J, Takhsha Ghahfarokhi M, *et al*. Development of 4D-bioprinted shape-morphing magnetic constructs for cartilage regeneration using a silk fibroin-gelatin bioink. *Cell Rep Phys Sci*. 2024;5(3):101819.

doi: 10.1016/j.xcrp.2024.101819

92. Fisher JG, Sparks EA, Khan FA, *et al*. Extraluminal distraction enterogenesis using shape-memory polymer. *J*

Pediatr Surg. 2015;50(6):938-942.

doi: 10.1016/j.jpedsurg.2015.03.013

93. Greener JG, Kandathil SM, Moffat L, Jones DT. A guide to machine learning for biologists. *Nat Rev Mol Cell Biol*. 2022;23(1):40-55.

doi: 10.1038/s41580-021-00407-0

94. Elbadawi M, Li H, Sun S, Alkahtani ME, Basit AW, Gaisford S. Artificial intelligence generates novel 3D printing formulations. *Appl Mater Today*. 2024;36:102061.

doi: 10.1016/j.apmt.2024.102061

95. Chen B, Dong J, Ruelas M, *et al*. Artificial intelligence-assisted high-throughput screening of printing conditions of hydrogel architectures for accelerated diabetic wound healing. *Adv Funct Mater*. 2022;32(38):2201843.

doi: 10.1002/adfm.202201843

96. Kim KY, Ryu J, Kang J, *et al*. A conformable multimodal imaging marker for surgical navigation systems. *npj Flexible Electron*. 2026;10(1):24.

doi: 10.1038/s41528-025-00525-1

97. Bashir S, Hina M, Iqbal J, *et al*. Fundamental concepts of hydrogels: synthesis, properties, and their applications. *Polymers*. 2020;12(11):2702.

doi: 10.3390/polym12112702

98. Kim W, Kim G. Collagen/bioceramic-based composite bioink to fabricate a porous 3D hASCs-laden structure for bone tissue regeneration. *Biofabrication*. 2019;12(1):015007.

doi: 10.1088/1758-5090/ab436d

99. Huang KH, Chen CY, Chang CY, Chen YW, Lin CP. The synergistic effects of quercetin-containing 3D-printed mesoporous calcium silicate/calcium sulfate/poly-ε-caprolactone scaffolds for the promotion of osteogenesis in mesenchymal stem cells. *J Formos Med Assoc*. 2021;120(8):1627-1634.

doi: 10.1016/j.jfma.2021.01.024

100. Li X, Deng Q, Wang S, *et al*. Hydroxyethyl cellulose as a rheological additive for tuning the extrusion printability and scaffold properties. *3D Print Addit Manuf*. 2021;8(2):87-98.

doi: 10.1089/3dp.2020.0167

101. Bishop ES, Mostafa S, Pakvasa M, *et al*. 3-D bioprinting technologies in tissue engineering and regenerative medicine: current and future trends. *Genes Dis*. 2017;4(4):185-195.

doi: 10.1016/j.gendis.2017.10.002

102. Tripathi S, Mandal SS, Bauri S, Maiti P. 3D bioprinting and its innovative approach for biomedical applications. *MedComm*. 2023;4(1):e194.

doi: 10.1002/mco2.194

103. Zhao W, Hu C, Xu T. In vivo bioprinting: broadening the therapeutic horizon for tissue injuries. *Bioact Mater*. 2023;25:201-222.

doi: 10.1016/j.bioactmat.2023.01.018

104. Mirasadi K, Yousefi MA, Jin L, *et al*. 4D printing of magnetically responsive shape memory polymers: toward sustainable solutions in soft robotics, wearables, and biomedical devices. *Adv Sci*. 2025;13(15):e13091.

doi: 10.1002/advs.202513091

105. Liu K, Su Y, Wang X, *et al*. Achieving simultaneous enhancement of strength and ductility in Al matrix composites by employing the synergetic strengthening effect of micro- and nano-SiCps. *Composites, Part B*. 2023;248:110350.

doi: 10.1016/j.compositesb.2022.110350

106. Rahmatabadi D, Mirasadi K, Bayati A, *et al*. 4D printing thermo-magneto-responsive PETG-Fe3O4 nanocomposites with enhanced shape memory effects. *Appl Mater Today*. 2024;40:102361.

doi: 10.1016/j.apmt.2024.102361

107. Shi Y, Tang S, Yuan X, *et al*. In situ 4D printing of polyelectrolyte/magnetic composites for sutureless gastric perforation sealing. *Adv Mater*. 2024;36(34):2307601.

doi: 10.1002/adma.202307601